

# Universal Symmetry in Complex Network Control

Chen Zhao,<sup>1</sup> Wen-Xu Wang,<sup>1</sup> Yang-Yu Liu,<sup>2,3</sup> and Jean-Jacques Slotine<sup>4,5</sup>

<sup>1</sup>*School of Systems Science, Beijing Normal University, Beijing, 10085, P. R. China*

<sup>2</sup>*Channing Division of Network Medicine, Brigham and Women's Hospital,  
Harvard Medical School, Boston, Massachusetts 02115, USA*

<sup>3</sup>*Center for Complex Network Research and Department of Physics,  
Northeastern University, Boston, Massachusetts 02115, USA*

<sup>4</sup>*Nonlinear Systems Laboratory, Massachusetts Institute of Technology,  
Cambridge, Massachusetts, 02139, USA*

<sup>5</sup>*Department of Mechanical Engineering and Department of Brain and Cognitive Sciences,  
Massachusetts Institute of Technology,  
Cambridge, Massachusetts, 02139, USA*

## Abstract

Major advances have been made recently towards understanding how to control large networks by acting only on a small subset of their elements, illuminating the impact of a network's topology on its controllability. Yet, a detailed understanding of the synergies between network topology and intrinsic individual dynamics is still lacking. Here we offer a theoretical framework to evaluate the controllability of complex networked systems with particular interest in the diversity of dynamic units characterized by different types of individual dynamics. Surprisingly, we find a universal symmetry accounting for the invariance of controllability with respect to exchanging the densities of any two different types of dynamic units, irrespective of the network topology. The highest controllability arises at the global symmetry point, at which different types of dynamic units have the same density. These findings have important implications for devising effective and sparse controllers of complex networked systems in a wide range of fields.

Due to the paramount importance of controlling complex networked systems, the recent development of structural-controllability framework [1] has triggered a burst of research activities [2–13]. Previous works typically focus on the effect of network topology rather than the individual dynamics of nodes on our ability to steer a complex network to any desired final state [5–11], as quantified by the minimum number of driver nodes on which independent input signals need to be imposed [1]. While the intrinsic individual dynamics can be incorporated in the network model, it would be more natural and fruitful to consider their effect separately. Indeed, in studying complex networked systems consisting of dynamic units characterized by individual dynamics, major new insights can be obtained by analyzing the role of diversity and similarity of the dynamic units. This will offer a more realistic characterization of real-world networked systems. Although previous works have attempted to explore the effect of individual dynamics on controllability [1, 6], they are still based on the structural controllability framework, assuming completely independent individual dynamics. The lack of a theoretical tool beyond structural controllability precluded us from understanding how network topology and individual dynamics jointly affect a system’s controllability.

The exact-controllability framework [14] introduced recently enables us to systematically explore the role of individual dynamics in controlling complex systems with arbitrary network topology. We consider prototypical linear forms of individual dynamics (from first-order to high-orders) that can be incorporated within the network representation of the whole system in a unified matrix form. The natural diversity of individual dynamics prompts us to consider different types of dynamic units in a network to better mimic real-world situations. This paradigm leads to the discovery of a universal symmetry of controllability: if we exchange the fractions of any two types of dynamic units, the system’s controllability remains the same. This exchange-invariant property gives rise to a global symmetry point, at which the highest controllability emerges. This symmetry-induced optimal controllability holds for any network topology and various categories of individual dynamics. We substantiate these findings numerically in both model and real networks.

## Controllability measurement

Structural controllability theory (SCT) [1, 15] is generally applicable to directed networks characterized by structural matrices in which the elements are either zeros or independent free parameters. In the presence of individual dynamics, the given parameters of individual dynamics might violate the requirement of structural matrices, e.g., two nodes share the same individual dynamics will yield the same matrix elements. This forces us to employ the recently developed exact-controllability theory as an alternative approach to address the problem.

Exact-controllability theory (ECT) [14] claims that for arbitrary network topology and link weights characterized by the state matrix  $A \in \mathbb{R}^{N \times N}$  in canonical linear time-invariant systems, the minimum number of driver nodes (denoted as  $N_D$ ) required to be controlled by imposing independent signals to fully control the system is given by the maximum geometric multiplicity  $\max_i \{\mu(\lambda_i)\}$  of  $A$ ’s eigenvalues  $\{\lambda_i\}$ . Here  $\mu(\lambda_i) \equiv N - \text{rank}(\lambda_i I_N - A)$  is the geometric multiplicity of the eigenvalue  $\lambda_i$  and  $I_N$  is the identity matrix. Calculating all the eigenvalues of  $A$  and subsequently counting their geometric multiplicities are generally applicable but

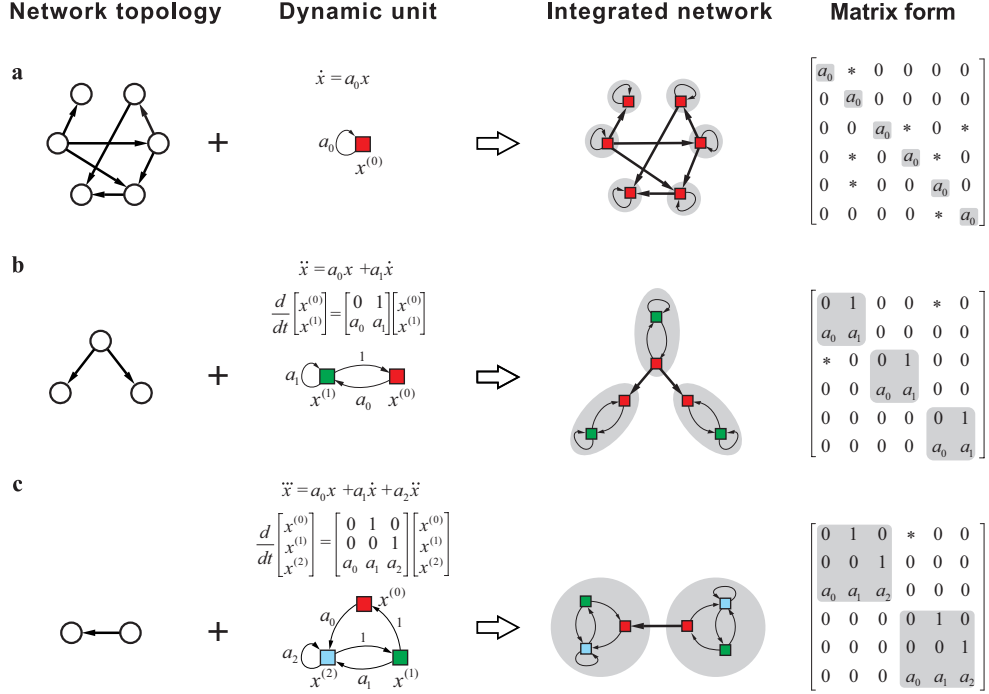


FIG. 1: **Integration of network topology and intrinsic individual dynamics.** 1st-order (a), 2nd-order (b) and 3rd-order (c) individual dynamics. For a  $d$ th-order individual dynamics  $x^{(d)} = a_0 x^{(0)} + a_1 x^{(1)} + \dots + a_{d-1} x^{(d-1)}$ , we denote each order by a colored square and the couplings among orders are characterized by links or self-loops. This graphical representation allows individual dynamics to be integrated with their coupling network topology, giving rise to a unified matrix that reflects the dynamics of the whole system. In particular, each dynamic unit in the unified matrix corresponds to a diagonal block and the nonzero elements (denoted by  $*$ ) apart from the blocks stand for the couplings among different dynamic units. Therefore, the original network consisting of  $N$  nodes with order  $d$  is represented in a  $dN \times dN$  matrix.

computationally prohibitive for large networks. If  $A$  is symmetric, e.g., in undirected networks,  $N_D$  is simply given by the maximum algebraic multiplicity  $\max_i \{\delta(\lambda_i)\}$ , where  $\delta(\lambda_i)$  denotes the degeneracy of eigenvalue  $\lambda_i$ . Calculating  $N_D$  in the case of symmetric  $A$  is more computationally affordable than in the asymmetric case. Note that for structured systems where the elements in  $A$  are either fixed zeros or free independent parameters, ECT offers the same results as that of the SCT [14].

### Controllability associated with first-order individual dynamics

We first study the simplest case of first-order individual dynamics  $\dot{x}_i = a_0 x_i$ . The dynamical equations of a linear time-invariant control system associated with first-order individual dynamics [16] can be written as

$$\dot{\mathbf{x}} = \Lambda \mathbf{x} + A \mathbf{x} + B \mathbf{u} = \Phi \mathbf{x} + B \mathbf{u}, \quad (1)$$

where the vector  $\mathbf{x} = (x_1, \dots, x_N)^T$  captures the states of  $N$  nodes,  $\Lambda \in \mathbb{R}^{N \times N}$  is a diagonal

matrix representing intrinsic individual dynamics of each node,  $A \in \mathbb{R}^{N \times N}$  denotes the coupling matrix or the weighted wiring diagram of the networked system, in which  $a_{ij}$  represents the weight of a directed link from node  $j$  to  $i$  (for undirected networks,  $a_{ij} = a_{ji}$ ).  $\mathbf{u} = (u_1, u_2, \dots, u_M)^T$  is the input vector of  $M$  independent signals,  $B \in \mathbb{R}^{N \times M}$  is the control matrix, and  $\Phi \equiv \Lambda + A$  is the state matrix. Without loss of generality, we assume  $\Lambda$  is a “constant” matrix over the field  $\mathbb{Q}$  (rational numbers), and  $A$  is a structured matrix over the field  $\mathbb{R}$  (real numbers). In other words, we assume all the entries in  $\Phi$  have been rescaled by the individual dynamics parameters. The resulting state matrix  $\Phi$  is usually called a mixed matrix with respect to  $(\mathbb{Q}, \mathbb{R})$  [17]. The first-order individual dynamics in  $\Phi$  is captured by self-loops in the network representation of  $\Phi$  (see Fig. 1a).  $N_D$  can then be determined by calculating the maximum geometric multiplicity  $\max_i \{\mu(\lambda_i)\}$  of  $\Phi$ 's eigenvalues.

We study two canonical network models (Erdős-Rényi and Scale-free) with random edge weights and a  $\rho_s$  fraction of nodes associated with identical individual dynamics (i.e., self-loops of identical weights). As shown in Fig. 2a,b, the fraction of driver nodes  $n_D \equiv N_D/N$  is symmetric about  $\rho_s = 0.5$ , regardless of the network topology. (Note that this is in sharp contrast to the prediction of structural control theory in case of independent self-loop weights where  $n_D$  monotonically decreases as  $\rho_s$  augments and eventually  $\rho_s = 1$  leads to  $n_D = 1/N$ , implying that a single driver node can fully control the whole network.) The symmetry can be theoretically predicted (see Methods). An immediate but counterintuitive consequence from the symmetry is that  $n_D$  in the absence of self-loops is exactly the same as the case that each node has a self-loop with identical weight. This is a direct consequence of Kalman's rank condition for controllability [18]:

$$\text{rank}[B, AB, \dots, A^{N-1}B] = \text{rank}[B, (A + w_s I_N)B, \dots, (A + w_s I_N)^{N-1}B], \quad (2)$$

where the left and the right hand sides are the rank of controllability matrix in the absence and full of identical self-loops, respectively.

The presence of two types of nonzero self-loops  $s_2$  and  $s_3$  leads to even richer behavior of controllability. If the three types of self-loops (including self-loops of zero weights) are randomly distributed at nodes, the impact of their fractions on  $n_D$  can be visualized by mapping the three fractions into a 2D triangle, as shown in Fig. 2e. We see that  $n_D$  exhibits symmetry in the triangle and the minimum  $n_D$  occurs at the center that represents identical fractions of the three different self-loop types. The symmetry-induced highest controllability can be generalized to arbitrary number of self-loops. Assume there exist  $n$  types of self-loops  $s_1, \dots, s_n$  with weights  $w_s^{(1)}, \dots, w_s^{(n)}$ , respectively, we have

$$N_D = N - \min_i \left\{ \text{rank}(\Phi - w_s^{(i)} I_N) \right\} \quad (3)$$

for sparse networks with random weights. An immediate prediction of Eq. (3) is that  $N_D$  is primarily determined by the self-loop with the highest density, simplifying Eq. (3) to be  $N_D = N - \text{rank}(\Phi - w_s^{\max} I_N)$ , where  $w_s^{\max}$  is the weight of the prevailing self-loop. Using Eq. (3) and the fact that  $\Phi$  is a mixed matrix, we can rigorously prove that  $N_D$  remains unchanged if we exchange the densities of any two types of self-loops (see Methods), accounting for the symmetry of  $N_D$  for arbitrary types of self-loops. Due to the dominance of  $N_D$  by the self-loop with the highest density and the exchange-invariance of  $N_D$ , the highest controllability with the lowest value of  $N_D$  emerges when distinct self-loops are of the same density.

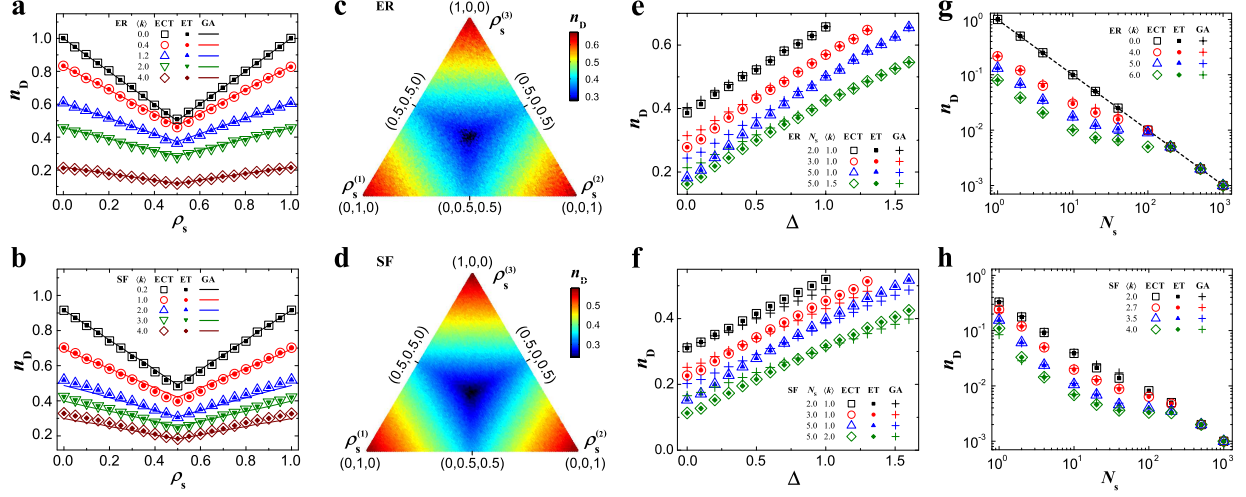


FIG. 2: **Controllability of networks with 1st-order individual dynamics.** **a-b**, controllability measure  $n_D$  in the presence of a single type of nonzero self-loops with fraction  $\rho_s$  for random (ER) networks (**a**) and scale-free (SF) networks (**b**) with different average degree  $\langle k \rangle$ . **c-d**,  $n_D$  of ER (**c**) and SF networks (**d**) with three types of self-loops  $s_1$ ,  $s_2$  and  $s_3$  with density  $\rho_s^{(1)}$ ,  $\rho_s^{(2)}$  and  $\rho_s^{(3)}$ , respectively. The color bar denotes the value of  $n_D$  and the coordinates in the triangle stands for  $\rho_s^{(1)}$ ,  $\rho_s^{(2)}$  and  $\rho_s^{(3)}$ . **e-f**,  $n_D$  as a function of the density heterogeneity of self-loops ( $\Delta$ ) for ER (**e**) and SF (**f**) networks. **g-h**,  $n_D$  as a function of the number of different types of self-loops for ER (**g**) and SF (**h**) networks. ECT denotes the results obtained from the exact controllability theory, ET denotes the results obtained from the efficient tool and GA denotes the results obtained from the graphical approach. The dotted line in (**g**) is  $n_D = 1/N_s$ . The networks are described by structured matrix  $A$  and their sizes in (**a**)-(**d**) are 2000 and that in (**e**)-(**h**) are 1000. The results from ECT and ET are averaged over 30 different realizations, and those from GA are over 200 realizations.

To validate the symmetry-induced highest controllability predicted by our theory, we quantify the density heterogeneity of self-loops as follows:

$$\Delta \equiv \sum_{i=1}^{N_s} \left| \rho_s^{(i)} - \frac{1}{N_s} \right|, \quad (4)$$

where  $N_s$  is the number of different types of self-loops (or the diversity of self-loops). Note that  $\Delta = 0$  if and only if all different types of self-loops have the same density, i.e.,  $\rho_s^{(1)} = \rho_s^{(2)} = \dots = \rho_s^{(N_s)} = \frac{1}{N_s}$ , and the larger value of  $\Delta$  corresponds to more diverse case. Figure 2e,f shows that  $n_D$  monotonically increases with  $\Delta$  and the highest controllability (lowest  $n_D$ ) arises at  $\Delta = 0$ , in exact agreement with our theoretical prediction. Figure 2g,h display  $n_D$  as a function of  $N_s$ . We see that  $n_D$  decreases as  $N_s$  increases, suggesting that the diversity of individual dynamics facilitates the control of a networked system. When  $N_s = N$  (i.e., all the self-loops are independent),  $n_D = 1/N$ , which is also consistent with the prediction of structural control theory [1].

## Controllability for high-order individual dynamics

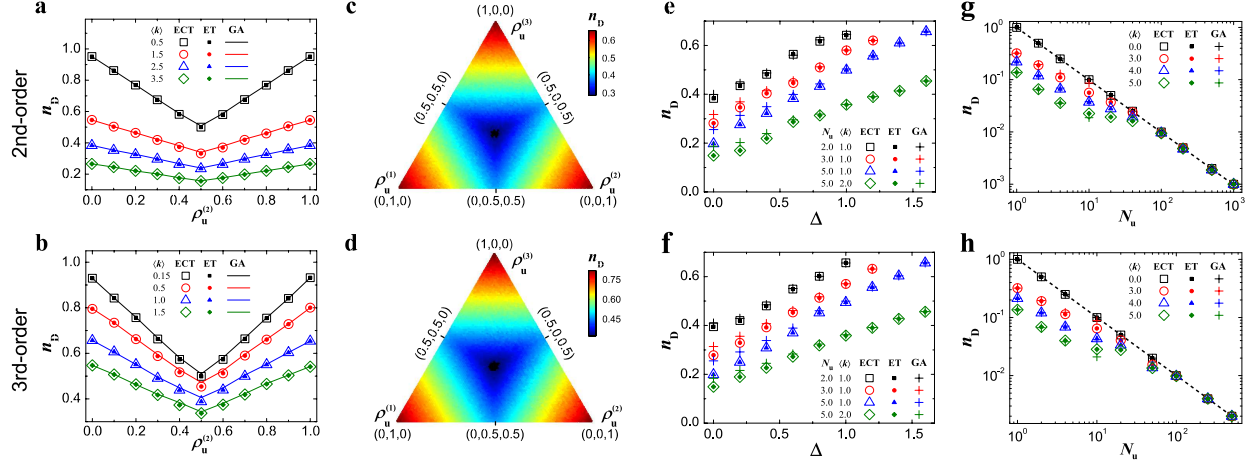


**FIG. 3: The controllability of networks with high-order individual dynamics.** **a-b**, controllability measure  $n_D$  in the presence of two types of dynamic units with density  $\rho_u^{(1)}$  and  $\rho_u^{(2)}$  belonging to the 2nd-order dynamic units (**a**) and 3rd-order dynamic units (**b**) for ER random networks with different average degree  $\langle k \rangle$ . **c-d**,  $n_D$  in the presence of three types of dynamic units with density  $\rho_u^{(1)}$ ,  $\rho_u^{(2)}$  and  $\rho_u^{(3)}$  belonging to the 2nd-order dynamic units (**c**) and 3rd-order dynamic units (**d**) for ER random networks. The triangle has the same meaning as that in Fig. 2. **e-f**,  $n_D$  as a function of the density heterogeneity ( $\Delta$ ) for 2nd-order (**e**) and 3rd-order (**f**) dynamic units on ER random networks. **g-h**,  $n_D$  as a function of the number  $N_u$  of different dynamic units subject to 2nd-order (**g**) and 3rd-order (**h**). The dotted line in (**g**) and (**h**) is  $n_D = 1/N_u$ . The network size of the 2nd-order dynamic units is 1000 and that of the 3rd-order dynamic units is 500. The networks are described by structured matrices  $A$ . The results from ECT and ET are averaged over 30 different realizations, and those from GA are over 200 realizations.

In some real networked systems, dynamic units are captured by high-order individual dynamics, prompting us to check if the universal symmetry-induced highest controllability still holds for higher-order individual dynamics. The graph representation of dynamic units with 2nd-order dynamics is illustrated in Fig. 1b. In this case, the eigenvalues of the dynamic unit's state matrix  $\begin{pmatrix} 0 & 1 \\ a_0 & a_1 \end{pmatrix}$  plays a dominant role in determining  $N_D$ . For two different units as distinguished by distinct  $(a_0 \ a_1)$  one can show that their state matrices almost always have different eigenvalues, except for some pathological cases of zero measure that occur when the parameters satisfy certain accidental constraints. The eigenvalues of dynamic unit's state matrix take over the roles of self-loops in the 1st-order dynamics, accounting for the following formulas for sparse networks

$$N_D = 2N - \min_i \left\{ \text{rank}(\Phi - \lambda^{(i)} I_{2N}) \right\}, \quad (5)$$

where  $\lambda^{(i)}$  is either one of the two eigenvalues of type- $i$  dynamic unit's state matrix. The formula implies that  $N_D$  is exclusively determined by the prevailing dynamic unit. The universal symmetry of  $N_D$ , i.e., exchanging the densities of any types of dynamic units does not alter  $N_D$  (see Methods), and the emergence of highest controllability at the global symmetry point can be similarly proved

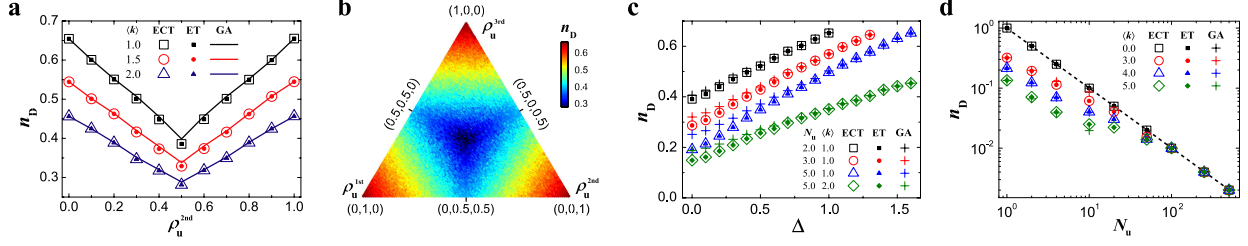


**FIG. 4: The controllability of networks consisting of a mixture of dynamic units with different orders.** **a**,  $n_D$  as a function of the density  $\rho_u^{2nd}$  of the 2nd-order dynamic unit incorporated with the 1st-order dynamic units. **b**,  $n_D$  as a function of the densities  $\rho_u^{1st}$ ,  $\rho_u^{2nd}$  and  $\rho_u^{3rd}$  of dynamic units associated with different orders. **c**,  $n_D$  as a function of the density heterogeneity,  $\Delta$ , for a mixture of dynamic units from 1st- to 3rd-order. **d**,  $n_D$  as a function of the number  $N_u$  of a mixture of different dynamic units from 1st- to 3rd-order. The number of dynamic units in (a)-(d) is 500 and ER random networks described by structural matrices are used. In (b), the average degree  $\langle k \rangle = 1$ . The dotted line in (d) is  $n_D = 1/N_u$ . Each data point is obtained by averaging over 100 independent realizations.

as we did in the case of 1st-order individual dynamics.

The 3rd-order individual dynamics are graphically characterized by a dynamic unit composed of three nodes (Fig. 1c), leading to a  $3N \times 3N$  state matrix (Fig. 1c). We can generalize Eq. (5) to arbitrary order of individual dynamics:

$$N_D = dN - \min_i \left\{ \text{rank}(\Phi - \lambda_d^{(i)} I_{dN}) \right\}, \quad (6)$$

where  $d$  is the order of the dynamic unit,  $\lambda_d^{(i)}$  is any one of the  $d$  eigenvalues of type- $i$  dynamic units and  $I_{dN}$  is the identity matrix of dimension  $dN$ . In analogy with the simplified formula for the 1st-order dynamics, insofar as a type of individual dynamics prevails in the system, Eq (6) is reduced to  $N_D = dN - \text{rank}(\Phi - \lambda_d^{\max} I_{dN})$ , where  $\lambda_d^{\max}$  is one of the eigenvalues of the prevailing dynamic unit's state matrix. The universal symmetry of controllability and the highest controllability occurs at the global symmetry point can be proved for individual dynamics of any order and arbitrary network topology. Fig. 3 displays the results for 2nd- and 3rd-order individual dynamics, where the density heterogeneity for high-order dynamic units is defined as  $\Delta \equiv \sum_{i=1}^{N_u} |\rho_u^{(i)} - 1/N_u|$ ,  $N_u$  is the number of different dynamic units and  $\rho_u^{(i)}$  is the density of type- $i$  dynamic unit.

We have also explored the mixture of individual dynamics with different orders, finding the symmetry of  $n_D$  and the highest controllability at the global symmetry point, in agreement with those found in the networks with single-order individual dynamics (see Fig. 4).

### The symmetry of controllability in real networks

We also explore the universal symmetry of controllability, for three classes of real networks: food webs [19–21], social networks [22–30] and power grids [31–35]. In food webs, individual dynamics are assumed to be first-order that capture the birth/death rate of species. For epidemic spreading on social networks, first-order individual dynamics can be associated with the curing

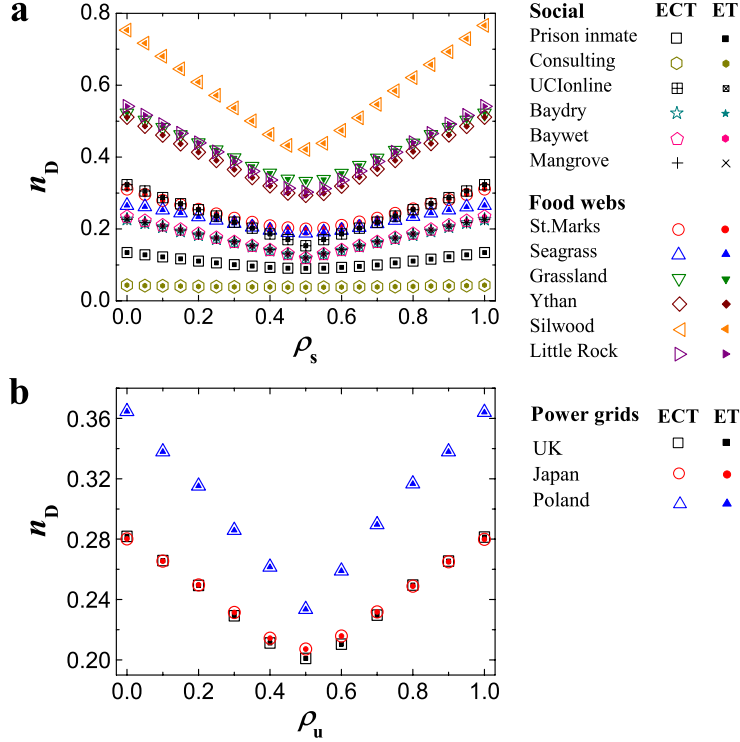


FIG. 5: **The controllability of real networks.** **a**,  $n_D$  as a function of the fraction  $\rho_s$  of one of two types of dynamic units in 1st order (**a**) and 2nd order (**b**). The results of each real network is the average over 500 independent realizations of random distributions of two types of dynamic units by using the ECT and ET. The 1st-order individual dynamics are appropriate for social networks and food webs and the 2nd-order ones are typical in power grids. For data sources and references.

rates of individuals. In power grids, individual dynamics can be typically described by the 2nd-order generator equation [33]. For simplicity but without loss of generality, we concentrate on two different types of individual dynamics and the coefficients of each type are assigned random numbers. This may also be viewed as a simplified model of systems with a slow, dominant time-scale, combined with faster dynamics. We represent the coupling networks by structural matrices due to our inherently incomplete knowledge of the link weights.  $n_D$  of the real networks is shown in Fig. 5. The universal symmetry and the highest controllability at the symmetry point are shared by all studied real networks, manifesting the generality of our theoretical prediction. We have tested more than two types of individual dynamics, for which the universal finding maintains in the real networks. It is noteworthy that although network topology does not break the symmetry phenomena qualitatively, it does influence the value of  $n_D$ , implying that the controllability of a complex network system is the result of the joint effect of individual dynamics and network topology.

## Discussion



In summary, we map individual dynamics into dynamic units that can be integrated into the matrix representation of the system, offering a general paradigm to explore the joint effect of individual dynamics and network topology on the system's controllability. The paradigm leads to a striking discovery: the universal symmetry of controllability as reflected by the invariance of controllability with respect to exchanging the fractions of any two different types of individual dynamics, and the emergence of highest controllability at the global symmetry point. These findings generally hold for arbitrary networks and individual dynamics of any order. The symmetry-induced highest controllability has immediate implications for devising and optimizing the control of complex systems by for example, perturbing individual dynamics to approach the symmetry point without the need to adjust network structure.

The theoretical paradigm and tools developed here also allow us to address a number of questions, answers to which could offer further insights into the control of complex networked systems. For example, similar individuals are often accompanied by dense inner connections among them, accounting for the widely observed communities with relatively sparse connections among them in natural and social systems. How such structural property in combination with the similarity and diversity of individual dynamics impacts control is worthy of exploration. Despite the advantage of our tools compared to the other methods in literature, the network systems that we can address are still the tip of the iceberg, raising the need of new tools based on network science, statistic physics and control theory. At the present, we are incapable of tackling general nonlinear dynamical systems, which is extremely challenging not only in complex networks but also in the canonical control theory for simple systems. Nevertheless, our approach, we hope, will inspire further interest from physicists and other scientists towards achieving ultimate control of complex networked systems.

- 
- [1] Liu, Y.-Y., Slotine, J.-J. & Barabási, A.-L. Controllability of complex networks. *Nature* **473**, 167-173 (2011).
  - [2] Nepusz, T. & Vicsek, T. Controlling edge dynamics in complex networks. *Nature Phys.*, **8**, 568-573 (2012).
  - [3] Yan, G., Ren, J., Lai, Y.-C., Lai, C.-H. & Li, B. Controlling complex networks: how much energy is needed? *Phys. Rev. Lett.* **108**, 218703 (2012).
  - [4] Liu, Y.-Y., Slotine, J.-J. & Barabási, A.-L. Control centrality and hierarchical structure in complex networks. *PLoS ONE* **7**(9):e44459. doi:10.1371/journal.pone.0044459.
  - [5] Wang, W.-X., Ni, X., Lai, Y.-C. & Grebogi, C. Optimizing controllability of complex networks by minimum structural perturbations. *Phys. Rev. E* **85**, 026115 (2012).
  - [6] Cowan, N. J., Chastain, E. J., Vilhena, D. A., Freudenberg, J. S. & Bergstrom, C. T. Nodal dynamics, not degree distributions, determine the structural controllability of complex networks. *PLoS ONE* **7**, e38398 (2012).
  - [7] Tang, Y., Gao, H., Zou, W. & Kurths, J. Identifying controlling nodes in neuronal networks in different scales. *PLoS ONE* **7**, e41375 (2012).
  - [8] Gutiérrez, R., Sendiña-Nadal, I., Zanin, M., Papo, D. & Boccaletti, S. Targeting the dynamics of

- complex networks. *Sci. Rep.* **2**, 396 (2012).
- [9] Wang, B., Gao, L. & Gao, Y. Control range: a controllability-based index for node significance in directed networks. *J. Stat. Mech.: Theor. Exp.* **2012**, P04011 (2012).
- [10] Pósfai, M., Liu, Y.-Y., Slotine, J.-J. & Barabási, A.-L. Effect of correlations on network controllability. *Sci. Rep.* **3**, 1067 (2013).
- [11] Jia, T., Liu, Y.-Y., Csóka, E., Pósfai, M., Slotine, J.-J. & Barabási, A.-L. Emergence of bimodality in controlling complex networks. *Nature Commun.* **4**, 2002 (2013).
- [12] Liu, Y.-Y., Slotine, J.-J. & Barabási, A.-L. Observability of complex systems. *Proc. Natl Acad. Sci.* **110**, 2460-2465 (2013).
- [13] Sun, J. & Motter, A. E. Controllability transition and nonlocality in network control. *Phys. Rev. Lett.* **110**, 208701 (2013).
- [14] Yuan, Z., Zhao, C., Di, Z., Wang, W.-X. & Lai, Y.-C. Exact controllability of complex networks. *Nature Commun.* **4**, 2447 (2013).
- [15] C. T. Lin, *IEEE Trans. Autom. Control* **19**, 201 (1974).
- [16] Slotine, J.-J. & Li, W. *Applied Nonlinear Control* (Prentice-Hall, 1991).
- [17] Murota, k. *Matrices and Matroids for Systems Analysis* (Springer Heidelberg Dordrecht London, New York, USA, 2010).
- [18] Kalman, R. E. Mathematical description of linear dynamical systems. *J. Soc. Indus. Appl. Math. Ser. A* **1**, 152-192 (1963).
- [19] May, R. M. Simple mathematical models with very complicated dynamics. *Nature* **261**, 459 (1976).
- [20] Hofbauer, J. & Sigmund, K. *Evolutionary Games and Population Dynamics* (Cambridge Univ. Press, Cambridge, UK, 1998).
- [21] Turchin, P. *Complex Population Dynamics: a Theoretical/Empirical Synthesis* (Princeton Univ. Press, Princeton, NJ, 2003)
- [22] Anderson, R. M. & May, R. M. *Infectious Diseases of Humans: Dynamics and Control* (Oxford Univ. Press, Oxford, 1992).
- [23] Boguná, M., Pastor-Satorras, R. & Vespignani, A. Absence of epidemic threshold in scale-free networks with degree correlations. *Phys. Rev. Lett.* **90**, 028701 (2003).
- [24] Parshani, R., Carmi, S. & Havlin, S. Epidemic threshold for the susceptible-infectious-susceptible model on random networks. *Phys. Rev. Lett.* **104**, 258701 (2010).
- [25] Castellano, C. & Pastor-Satorras, R. Thresholds for epidemic spreading in networks. *Phys. Rev. Lett.* **105**, 218701 (2010).
- [26] Colizza, V., Barrat, A., Barthélemy, M. & Vespignani, A. The role of the airline transportation network in the prediction and predictability of global epidemics. *Proc. Natl Acad. Sci. USA* **103**, 2015-2020 (2006).
- [27] Hufnagel, L., Brockmann, D. & Geisel, T. Forecast and control of epidemics in a globalized world. *Proc. Natl Acad. Sci. USA* **101**, 15124-15129 (2004).
- [28] Colizza, V., Pastor-Satorras, R. & Vespignani, A. Reaction-diffusion processes and metapopulation models in heterogeneous networks. *Nature Phys.* **3**, 276-282 (2007).
- [29] Wang, B., Cao, L., Suzuki, H. & Aihara, K. Safety-Information-Driven Human Mobility Patterns with Metapopulation Epidemic Dynamics. *Sci. Rep.* **2**, 887 (2012).
- [30] Gatto, M., Mari, L., Bertuzzo, E., Casagrandi, R., Righetto, L., Rodriguez-Iturbe, I. & Rinaldo, A.

- Generalized reproduction numbers and the prediction of patterns in waterborne disease. *Proc. Natl Acad. Sci. USA* **109**, 19703-19708 (2012).
- [31] Strogatz, S. H. *SYNC: The Emerging Science of Spontaneous Order* (Hyperion, 2003).
- [32] Grainger, J. J. & Stevenson, W. D. Jr *Power System Analysis* (McGraw-Hill, 2004).
- [33] Anderson, P. M. & Fouad, A. A. *Power System Control and Stability* 2nd edn (IEEE Press-Wiley Interscience, 2003).
- [34] Rohden, M., Sorge, A., Timme, M. & Witthaut, D. Self-organized synchronization in decentralized power grids. *Phys. Rev. Lett.* **109**, 064101 (2012).
- [35] Motter, A. E., Myers, S. A., Anghel, M. & Nishikawa, T. Spontaneous synchrony in power-grid networks. *Nature Phys.* **9**, 191-197 (2013).
- [36] Horn, R. A. & Johnson, C. R. *Matrix Analysis*(Cambridge University Press, Cambridge, UK, 1985).
- [37] Strang, G. *Linear Algebra and Its Applications* (4th ed.) (Thomson Brooks/Cole, Belmont, CA, USA, 2006).
- [38] Papoulis, A. & Pillai, S. U. *Probability, Random Variables and Stochastic Processes* (3rd ed.) (McGraw-Hill, New York, USA, 2002).
- [39] Hautus, M. L. J. Controllability and observability conditions of linear autonomous systems, *Ned. Akad. Wetenschappen, Proc. Ser. A* **72**, 443-448 (1969).
- [40] Erdős, P. & Rényi, A. On the evolution of random graphs. *Publ. Math. Inst. Hung. Acad. Sci.* **5**, 17-61 (1960)
- [41] Barabási, A.-L. & Albert, R. Emergence of scaling in random networks. *Science* **286**, 509-512 (1999).